

# Static point-to-set correlations in glass-forming liquids

Ludovic Berthier and Walter Kob

Laboratoire Charles Coulomb, UMR 5221, CNRS and Université Montpellier 2, Montpellier, France

(Dated: January 26, 2013)

We analyze static point-to-set correlations in glass-forming liquids. The generic idea is to freeze the position of a set of particles in an equilibrium configuration and to perform sampling in the presence of this additional constraint. Qualitatively different geometries for the confining set of particles are considered and a detailed comparison of resulting static and dynamic correlation functions is performed. Our results reveal the existence of static spatial correlations not detected by conventional two-body correlators, which appear to be decoupled from, and shorter-ranged than, dynamical length scales characterizing dynamic heterogeneity. We find that the dynamics slows down dramatically under confinement, which suggests new ways to investigate the glass transition. Our results indicate that the geometry in which particles are randomly pinned is the best candidate to study static correlations.

PACS numbers: 05.10.-a, 05.20.Jj, 64.70.kj

The collective nature of the dynamics of supercooled liquids approaching the glass transition is well established [1]. A recent key advance was the study of multi-point dynamical correlation functions instead of traditional two-point correlation functions such as the intermediate scattering function. A central outcome is the determination of a *dynamical* length scale increasing by a factor of about 5-10 when glass-formers are cooled from normal liquid conditions to temperatures around the glass temperature  $T_g$ . This raises the question of the underlying existence of nontrivial *structural* correlations, which also grow when the glass transition is approached, and how they relate to dynamic ones [2]. However, just as two-time dynamic correlation functions do not detect directly dynamic heterogeneity, two-point density correlation functions (pair correlation functions) seem unable to capture the relevant structural correlations, as these functions only show a mild temperature dependence. There are proposals that three-body orientational order parameters might give insight for some specific glass-formers [3, 4], or that local geometric structures might be significant [5, 6], but *generic* methods to detect static order still need to be devised.

Recently, the idea emerged that some form of ‘amorphous order’ should develop in viscous liquids, which could be detected through ‘point-to-set’ correlation functions [7–11]. Point-to-set (PTS) correlations probe static multi-point correlations, since they are determined by fixing the position of a ‘set’ of  $k$  particles and measuring the probability to find a  $(k + 1)$ th particle at position  $\mathbf{r}_{k+1}$ . It can be hoped that if the geometry of the frozen set is well chosen, these multi-point functions yield spatial information without measuring how the correlation function depends on all its  $k + 1$  arguments. For a spherical cavity of radius  $d$ , for instance, one expects to detect a change of physical behavior when  $d$  interferes with the relevant structural length scale [8]. Although first motivated in the context of the random first order transition (RFOT) theory [12], the set-up is actually more general and does not rely on any hypothesis regarding the mi-

croscopic nature of the measured correlations. The generality of the approach thus strongly suggests that it is important to explore in detail these PTS correlations in different geometries for the set as well as for various models of glassy systems. Although reminiscent of studies of glass-formers in confined geometries [13], we emphasize that PTS correlations probe genuine *bulk* correlations, with no contribution from an external substrate [7, 14]. While difficult to implement for molecular systems, investigations along the lines suggested in the present work could be performed in colloidal materials where it is possible to freeze the position of a selected set of particles using for instance optical tweezers.

In this work, we show that PTS correlations can be detected using a broad variety of qualitatively distinct geometries, see Fig. 1, which all reveal information on static correlations not included in conventional pair correlations. As a first step, we present the results of computer simulations of a simple glass-former in which we

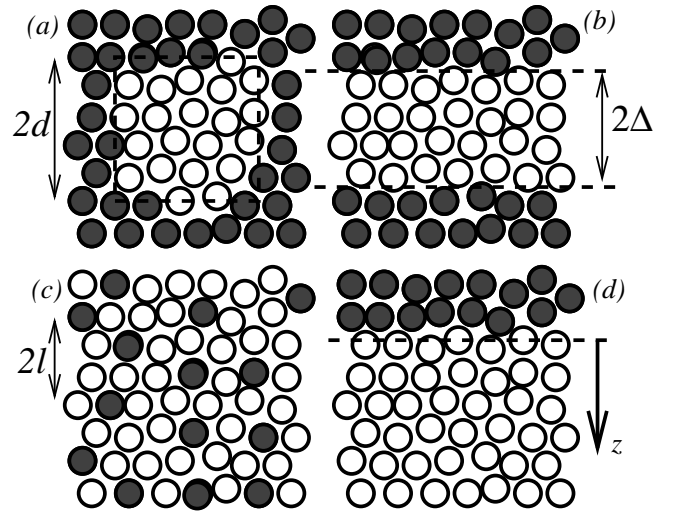


FIG. 1: Four qualitatively different geometries to investigate point-to-set correlations in glass-forming liquids.

investigate how the geometry of the pinned particles influences the measured correlations at a single state point. Our results suggest that the cavity geometry considered in earlier studies might not be the optimal choice to study static correlations. Another surprising outcome of our analysis is that static lengthscales appear to be decoupled from, and smaller than, dynamical lengthscales characterizing dynamic heterogeneity in the mildly supercooled regime typically studied in computer simulations.

For each of the geometries shown in Fig. 1 we first equilibrate a three dimensional bulk system composed of  $N$  particles. At  $t = 0$  we permanently pin  $k$  particles (filled circles in Fig. 1) whereas the remaining  $N - k$  particles (open circles) move as before. Since the pinned particles were chosen from the equilibrated fluid, the thermodynamics of the free particles is strictly unperturbed, provided an average is performed over both thermal fluctuations and different realizations of the pinning disorder [14, 15]. For the wall shown in Fig. 1d, the average density profile is for instance strictly constant,  $\langle \rho(z) \rangle = \rho_0$ , with no layering. We use constant temperature molecular dynamics simulations to study a 50:50 binary mixture of harmonic spheres with size ratio 1.4, all particles having the same mass  $m$  [16]. The unit of length is given by  $\sigma$ , the diameter of the small particles, the unit of time by  $\sqrt{m\sigma^2/\varepsilon}$ , where  $\varepsilon$  is the interaction strength, and temperature in units of  $10^{-4}\varepsilon$ , setting the Boltzmann constant  $k_B = 1.0$ . We work at fixed density  $\rho_0 = 0.675$ . For these parameters [17], slow dynamics sets in when  $T \lesssim 10$ , a fit to a mode-coupling divergence yields  $T_c \approx 5.2$ , and the harmonic spheres behave as quasi-hard spheres, as discussed in detail in Refs. [16]. Thus our system is a canonical model for studies of the glass transition phenomenon. As announced, we present a comparative study of the various confinement shown in Fig. 1 for a single, moderately low temperature,  $T = 8 > T_c$ , a temperature at which the intermediate scattering function of the bulk system already shows two-step relaxation.

In all cases we wish to answer the following question: How does the presence of a pinned set of particles affect the structure and dynamics of the remaining free particles? To quantify these effects we define two overlap functions, akin to the collective and self intermediate scattering functions. The collective overlap reads

$$Q(t) = \sum_i \langle n_i(t)n_i(0) \rangle / \sum_i \langle n_i(0) \rangle, \quad (1)$$

where the sum runs over the cells (of volume  $v \approx 0.53^3$ , comparable to the particle volume) of a cubic grid, and  $n_i(t) \in \{0, 1\}$  is the occupation number of cell  $i$  at time  $t$ . We set  $n_i = 0$  if cell  $i$  contains a pinned particle. The overlap  $Q(t)$  is close to 1 if configurations at time 0 and  $t$  are similar, but  $Q(t)$  is unaffected by particle exchanges. The long-time limit of the overlap,  $Q_\infty \equiv Q(t \rightarrow \infty)$ , provides direct information on static correlations. We

also define the single particle function

$$Q_{\text{self}}(t) = \sum_i \langle n_i^s(t)n_i^s(0) \rangle / \sum_i \langle n_i^s(0) \rangle, \quad (2)$$

where  $n_i^s(t) = 1$  if the same particle occupies the cell  $i$  at times 0 and  $t$ , and  $n_i^s(t) = 0$  otherwise.

We now describe the various geometries of Fig. 1. (a) Particles outside a cubic cavity of linear size  $2d$  are frozen. The overlaps are measured at the center of the cavity, using the  $4^3$  central cells to improve the statistics; 8 independent realizations are studied for each  $d$ . A similar (spherical) geometry has been studied in [10, 11]. (b) Particles outside the range  $0 < z < 2\Delta$  are frozen, such that the free particles are ‘sandwiched’ between two infinite walls separated by a distance  $2\Delta$ . The overlap is averaged over cells located in the plane parallel to the walls in the middle of the sandwich; 10 independent realizations are studied for each  $\Delta$ , with  $L_x = L_y = 13.68$ . (c) A finite fraction,  $c$ , of particles is randomly selected in the fluid, with a typical distance between them  $2l = c^{-1/3}$  [18]. The overlap is averaged over all cells. By using a large isotropic system,  $L = 16.3$ , only few realizations (typically 2-3) are needed to yield statistically accurate results. (d) Particles in the semi-infinite space  $z < 0$  are frozen. The overlap is averaged over cells belonging to planes parallel to the wall at distance  $z$  from it. This geometry has been studied in more detail (including different temperatures) in [17]. For (b) and (d) we also included a hard wall at the boundary between the wall(s) and the fluid to prevent free particles to penetrate the walls [14]. To perform quantitative comparisons, we define a ‘confining length’  $\xi$ , respectively as  $\xi = d, \Delta, l$ , or  $z$ : a smaller  $\xi$  means stronger confinement. Physically,  $\xi$  represents for each geometry the typical distance between the point where the overlap is measured to the pinned set of frozen particles. Note finally that geometry (a) is peculiar since the number of confined particles is always finite, while it scales with system size and diverges in the thermodynamic limit in cases (b-d).

In Fig. 2 we gather our results for the four geometries, both overlaps (1) and (2), and various degrees of confinement. In all geometries the time correlation functions have a similar qualitative behavior. When  $\xi \rightarrow \infty$ , bulk behaviour of the overlap  $Q(t)$  is recovered, with a two-step decay, and at long times a relaxation to the random value,  $Q_{\text{rand}} \approx 0.110595 \approx \rho_0 v$ . When confinement increases, the time dependence of  $Q(t)$  slows down, while the long-time limit increases,  $Q_\infty(\xi) > Q_{\text{rand}}$ . In practice we extract  $Q_\infty(\xi)$  by fitting the long-time decay of  $Q(t)$  to stretched exponential form. The quality of the fit is very good, as exemplified in Fig. 2b. In order to see that such a fit does indeed allow to obtain  $Q_\infty(\xi)$  with high precision, we show in Fig. 3 the time dependence of  $Q(t) - Q_{\text{rand}}$  on a logarithmic scale as well as the corresponding fits. Finally we note that the evolution of  $Q_{\text{self}}(t)$  is similar, showing a dramatic slowing down with increasing confinement, but its long-time limit is always zero.

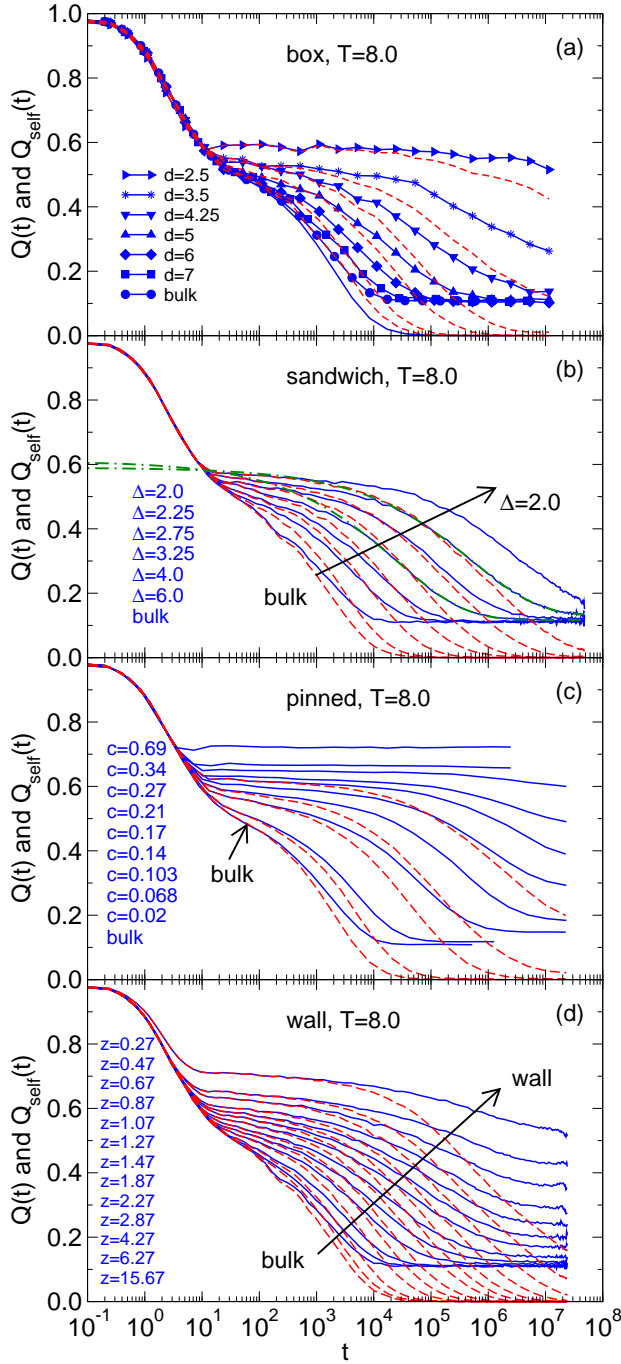


FIG. 2: Time dependence of the overlaps  $Q(t)$  (full lines) and  $Q_{\text{self}}(t)$  (dashed lines) for  $T = 8.0$ . The panels correspond to the four geometries of Fig. 1. In (b) we have also included the results of fits with a stretched exponential to the  $Q(t)$  data for  $\Delta = 2.25$  and  $\Delta = 3.25$  (dashed-dotted lines).

A comparison between both functions shows that  $Q(t)$  roughly reaches  $Q_{\infty}$  when  $Q_{\text{self}}(t)$  approaches zero, i.e. essentially when all particles have escaped the position they occupy at  $t = 0$ . Thus, when  $Q_{\infty} > Q_{\text{rand}}$ , non-random local density fluctuations persist even though particles diffuse and explore the available space. By mon-

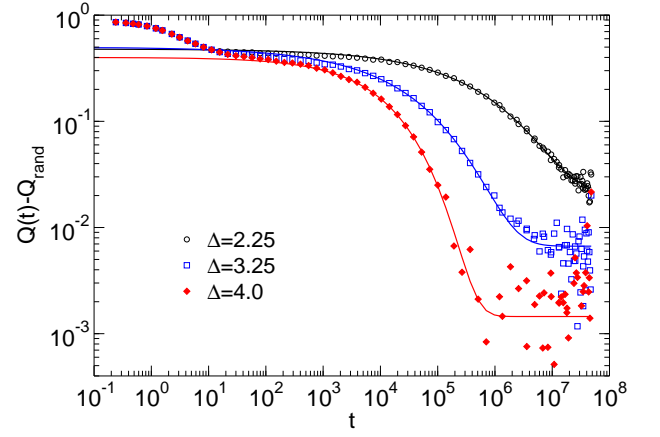


FIG. 3: Time dependence of the overlap  $Q(t) - Q_{\text{rand}}$  (symbols) and the stretched exponential fits (lines) for the sandwich geometry and different values of  $\Delta$ .

itoring the  $\xi$ -dependence of  $Q_{\infty}$ , we can quantify the amount of static order imposed by the confinement and have direct quantitative access to the influence of the set of frozen particles on the fluid structure to obtain bulk, equilibrium, many-body information not contained in pair correlations [7–11, 17].

From Fig. 2, we also conclude that measuring the evolution of the static overlap  $Q_{\infty}$  is more difficult than previously thought [8, 10, 19], because the dynamics slows down considerably with increasing confinement [14]. Whereas the bulk dynamics at  $T = 8$  corresponds to a moderately viscous state, there exists in all four geometries a maximal confinement above which  $Q(t)$  does not reach its long-time limit in the time window of our simulations, and hence large values of  $Q_{\infty}$  cannot be accessed. This difficulty gets even more pronounced at lower  $T$  [17], meaning that the measurement of point-to-set correlations closer to  $T_c$  is, at present, extremely challenging.

In Fig. 4, we present the evolution of the average overlap  $Q_{\infty}(\xi)$  as a function of the confining length  $\xi$  in all geometries (a), and the evolution of the corresponding relaxation times  $\tau(\xi)$  (b), defined from the time decay of  $Q_{\text{self}}(t)$  to the value  $1/e$ . In the latter figure we normalize the data by the bulk value  $\tau_{\infty} = \tau(\xi \rightarrow \infty)$ . The static profiles confirm that the average overlap becomes increasingly non-random by increasing the confinement since at a given confinement length we find that  $Q_{\infty}$  increases for the sequence pinned, wall, sandwich, box. Note that for the first three geometries the values of  $Q_{\infty}$  are similar, whereas the ones for the box are significantly larger. This indicates that the effect of confinement is highly non-linear. In cases (b) and (d) we find that the large  $\xi$  decay of  $Q_{\infty}$  is compatible with an exponential decay,  $Q_{\infty}(\xi) - Q_{\text{rand}} \approx \exp(-\xi/\xi_{\text{stat}})$ , which defines a PTS static lengthscale,  $\xi_{\text{stat}}$ . For geometry (d) this dependence holds for temperatures as low as  $T = 5.0 < T_c$  [17]. A compressed exponential decay was reported for a closed

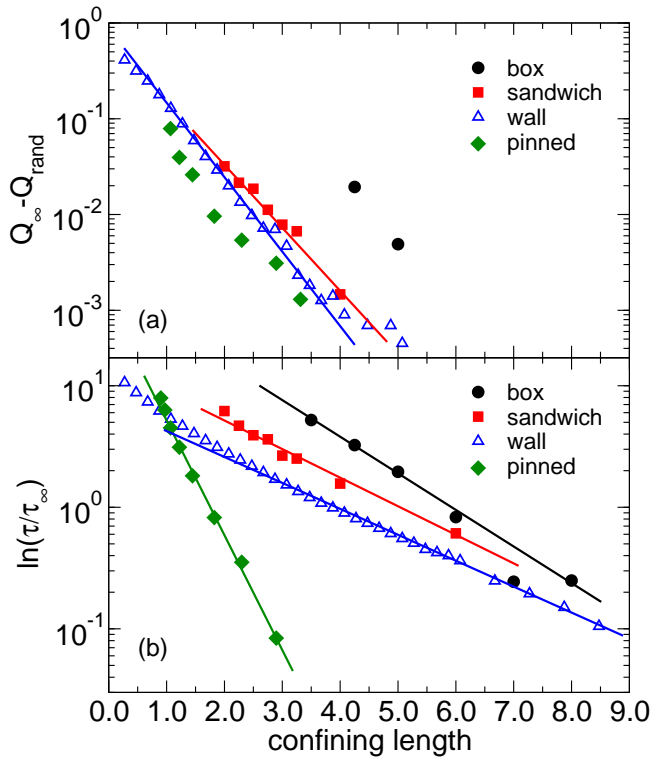


FIG. 4: a) Dependence of the overlap  $Q_\infty$  on the confining length for all geometries at  $T = 8$  (symbols) fitted with an exponential decay at long distances (straight lines). b) Relaxation time of the self overlap normalized by its bulk value.

cavity in Ref. [10], which is unfortunately the geometry for which our data is the most limited. For randomly pinned particles, one expects the non-random part of the overlap to scale as  $c = 1/\xi^3$  for large  $\xi$ , and an exponential decay is not expected in that case, which requires a separate analysis (see also [20]).

Regarding dynamics, we find that decreasing  $\xi$  at constant  $T$  leads to a strong slowing down of the dynamics for both self and collective quantities. In absolute values,  $\tau(\xi)$  strongly increases with the number of confining walls which shows that relaxation is non-linearly suppressed by adding more constraints. For a given confining length, pinned particles have of course much less impact on the dynamics as a single particle has obviously less effect than an entire wall. For the cavity (a), the slowing down is in fact so dramatic that the range of  $\xi$  where  $Q_\infty$  can be measured is very small: The overlap is too small when  $\xi$  is large, but dynamics is much too slow when  $\xi$  is small, which only leaves a narrow range to measure the static profile. We conclude that measuring PTS correlations in a closed cavity is in practice a difficult task in the interesting supercooled regime.

For a single wall,  $\tau(\xi)$  can be followed down to  $\xi \rightarrow 0$ , while for the other geometries small values of  $\xi$  are not accessible due to a much stronger slowing down. All dynamic profiles in Fig. 4b are well described by an exponential decay,  $\ln(\tau/\tau_\infty) \approx \exp(-\xi/\xi_{\text{dyn}})$  which directly

allows one to extract a dynamic correlation lengthscale  $\xi_{\text{dyn}}$  [14, 21]. In Ref. [17] we have explored its temperature dependence for a single wall and discussed how  $\xi_{\text{dyn}}$  relates to previous measures of dynamic lengthscales. From Fig. 4b we see that the slowing down of the dynamics is the least pronounced for the pinned geometry. Therefore we suggest that this geometry might be best suited best for the investigation of the  $T$ -dependence of static correlations.

By comparing the two panels in Fig. 4, it is obvious that for all geometries the dynamics seems to be affected over a broader range of confinement than statics, which suggests that, generically,  $\xi_{\text{dyn}} > \xi_{\text{stat}}$ . In fact we have frequently found parameters for which clear deviations from bulk dynamics are observed while the static overlap is still random, suggesting a clear decoupling between static and dynamic correlations. This decoupling is strong for a single wall and becomes less pronounced for randomly pinned particles. Our study thus seems to confirm [9, 17] that static correlation length scales are generically decoupled from dynamic ones and smaller, at least over the range of temperature we can explore numerically.

We finally discuss our results in a broader context. Theoretical progress on the glass problem is slowed by the lack of an obvious structural indicator to distinguish a glass from a fluid. It has only recently been realized that, in the framework of RFOT theory, the ‘ideal glass’ phase below the Kauzmann transition,  $T_K$ , is characterized by an infinite static PTS lengthscale [8, 9]. This implies for instance that below  $T_K$ , freezing a semi-infinite space as in Fig. 1d determines the position of the particles in the entire  $z > 0$  space [6]. Spatially extended static profiles, such as shown in Fig. 4, thus uniquely characterize fluids approaching the glass transition [10, 17], and do not provide valuable information for liquids at high temperatures.

Within RFOT theory, a static length  $\xi_{\text{RFOT}}(T)$  emerges from a spatial interpretation of the (mean-field) concept of metastable states [12]. This ‘mosaic’ length scale plays a role similar to that of a nucleation length scale in first order transitions, because it is set by the competition between the entropic gain of exploring different states and the energy cost of having interfaces between them [12]. This should be reflected, in the closed cavity of Fig. 1a, as a crossover between a small  $Q_\infty$  when  $d > \xi_{\text{RFOT}}$ , to a large  $Q_\infty$  when  $d < \xi_{\text{RFOT}}$ , since for decreasing confinement the surface tension eventually dominates [8]. A qualitatively similar crossover holds for geometries (b, c) as well, but not for a single wall in (d) where bulk behaviour with  $Q_\infty = Q_{\text{rand}}$  is recovered far from the wall and an interface must always be present.

In contrast to closed cavities, the crossover set by  $\xi_{\text{RFOT}}$  involves in geometries (b) and (c) a number of particles that diverges in the thermodynamic limit. This ‘crossover’ should therefore more properly be described as a genuine freezing transition towards an ideal glass phase where  $Q_\infty$  is large and density fluctuations do not

relax (see also [22]). A glass phase can then be approached either by decreasing  $T$  in the bulk, or by increasing the confinement at constant  $T$ , which opens exciting perspectives to study the glass transition. We are presently pursuing the exploration of the glass phase obtained at large pinning density, but the results go much beyond the theme of the present article and will be presented elsewhere. Our results also motivate further analysis of the phase diagram of viscous liquids in confined geometries (b, c). Analytical calculations for randomly pinned particles exist for hard sphere systems within mode-coupling theory [23], while the present results have motivated both an RFOT analysis [22] and some numer-

ical investigation [20]. Future work should characterize and compare in more detail the temperature evolution of the static and dynamic lengthscales introduced in this work beyond the case of the single wall studied in [17].

### Acknowledgments

We thank G. Biroli, C. Cammarota, D. Coslovich, R. Jack, J. Kurchan, D. Reichman, F. Sausset, G. Tarjus and the authors of [10] for discussions. W. K. is a member of the Institut universitaire de France.

- 
- [1] *Dynamical heterogeneities in glasses, colloids, and granular media*, Eds.: L. Berthier, G. Biroli, J.-P. Bouchaud, L. Cipelletti, and W. van Saarloos, (Oxford University Press, Oxford, 2011).
  - [2] L. Berthier and G. Biroli, *Rev. Mod. Phys.* **83**, 587 (2011).
  - [3] G. Tarjus, S. A. Kivelson, Z. Nussinov, and P. Viot, *J. Phys.: Condens. Matter* **17**, R1143 (2005).
  - [4] H. Tanaka, T. Kawasaki, H. Shintani, and K. Watanabe, *Nature Mater.* **9**, 324 (2010).
  - [5] D. Coslovich and G. Pastore, *J. Chem. Phys.* **127**, 124504 (2007).
  - [6] J. Kurchan and D. Levine, *J. Phys. A: Math. Theor.* **44**, 035001 (2011).
  - [7] A. Montanari and G. Semerjian, *J. Stat. Phys.* **125**, 22 (2006).
  - [8] J.-P. Bouchaud and G. Biroli, *J. Chem. Phys.* **121**, 7347 (2004).
  - [9] S. Franz and A. Montanari, *J. Phys. A: Math. Theor.* **40**, F251 (2007).
  - [10] A. Cavagna, T. S. Grigera, and P. Verrocchio, *Phys. Rev. Lett.* **98**, 187801 (2007); G. Biroli, J.-P. Bouchaud, A. Cavagna, T. S. Grigera, and P. Verrocchio, *Nature Phys.* **4**, 771 (2008).
  - [11] R. L. Jack and J. P. Garrahan, *J. Chem. Phys.* **123**, 164508 (2005).
  - [12] T. R. Kirkpatrick, D. Thirumalai, and P. G. Wolynes, *Phys. Rev. A* **40**, 1045 (1989).
  - [13] M. Alcoutlabi and G. B. McKenna, *J. Phys. Condens. Matter* **17**, R461 (2005).
  - [14] P. Scheidler, W. Kob, and K. Binder, *J. Phys. Chem. B* **108**, 6673 (2004), P. Scheidler, W. Kob, K. Binder, and G. Parisi, *Phil. Mag. B* **82**, 283 (2002).
  - [15] V. Krakoviack, *Phys. Rev. E* **82**, 061501 (2010).
  - [16] L. Berthier and T. A. Witten, *EPL* **86**, 10001 (2009); *Phys. Rev. E* **80**, 021502 (2009).
  - [17] W. Kob, S. Roldan-Vargas, and L. Berthier, *Nature Phys.* (in press); arXiv:1107.3928.
  - [18] K. Kim, *Europhys. Lett.* **61**, 790 (2003); S. Karmakar and I. Procaccia, arXiv:1105.4053.
  - [19] A. Cavagna, T. S. Grigera, and P. Verrocchio, arXiv:1006.3746.
  - [20] B. Charbonneau, P. Charbonneau, and G. Tarjus, arXiv:1108.2494.
  - [21] K. Watanabe, T. Kawasaki, and H. Tanaka, *Nature Mater.* **10**, 512 (2011).
  - [22] C. Cammarota and G. Biroli, arXiv:1106.5513
  - [23] V. Krakoviack, *Phys. Rev. Lett.* **94**, 065703 (2005); arXiv:1110.0606.